Title

Nonlinear seismic ground response analysis: code usage protocols and verification against vertical array data

Authors

Stewart, Jonathan P
Kwok, Annie O.L.

Publication Date

2008

Peer reviewed

Nonlinear Seismic Ground Response Analysis: Code Usage Protocols and Verification against Vertical Array Data

Jonathan P. Stewart[1], M. ASCE and Annie O.L. Kwok[2], M. ASCE

[1]Professor and Vice Chair, Dept. of Civil & Environmental Engr., Univ. of Calif., Los Angeles, 5731 Boelter Hall, Los Angeles, CA 90095; jstewart@seas.ucla.edu
[2] Project Engineer, Praad Geotechnical, Inc., 5465 S. Centinela Avenue, Los Angeles, CA 90066; AnnieOLKwok@engineering.ucla.edu

ABSTRACT: One-dimensional seismic ground response analyses are often performed using equivalent-linear procedures, which require few, generally well-known parameters. Nonlinear analyses have the potential to more accurately simulate soil behavior, but their implementation in practice has been limited because of poorly documented and unclear parameter selection and code usage protocols as well as inadequate documentation of the benefits of nonlinear modeling relative to equivalent linear modeling. Regarding code usage/parameter selection protocols, the following are described: (1) when input motions are from ground surface recordings, we show that the full outcropping motion should be used without converting to a "within" condition; (2) Rayleigh damping should be specified using at least two matching frequencies with a target level equal to the small strain soil damping; (3) the "target" soil backbone curves used in analysis can be parameterized to capture either the soil's dynamic shear strength when large-strain soil response is expected (strains approaching 1%), relatively small-strain response (i.e., $\gamma < 0.3\%$) as inferred from cyclic laboratory tests, or a hybrid of the two; (4) models used in nonlinear codes inevitably represent a compromise between the optimal fitting of the shapes of backbone and hysteretic damping curves, and we present two alternatives for model parameterization. The parameter selection and code usage protocols are tested by comparing predictions to data from vertical arrays. We find site amplification to be generally underpredicted at high frequencies and overpredicted at the elastic site period, where a strong local resonance occurs that is not seen in the data. We speculate that this bias results from over-damping.

INTRODUCTION

Nonlinear ground response analysis is seldom used in practice by non-expert users because parameter selection and code usage protocols are poorly documented and understood, the effect of parametric variability on the analysis results is generally unknown, and the benefits of nonlinear analysis relative to the widely-used equivalent-linear analysis are generally unquantified and unclear. We report results of a

benchmarking project for nonlinear ground response analysis codes organized through the Pacific Earthquake Engineering Research (PEER) center Lifelines program (Stewart et al. 2007). The objective of the project was to "de-mystify" nonlinear ground response analysis routines for practicing engineers by providing clear and well documented code usage protocols, to verify the codes as implemented with the usage protocols against vertical array data, and to investigate the differences between predictions provided by nonlinear and equivalent-linear analyses.

This paper provides an overview of the principal results of benchmarking project. The topics covered include the following:

1. Suppose that ground response analyses are to be performed using a given control motion accelerogram. We address whether that motion should be used as-recorded of if it should be modified to a "within" condition.
2. Most nonlinear codes utilize Rayleigh damping so that a finite level of damping is present regardless of the backbone curve. We address the manner by which Rayleigh damping should be specified.
3. Material behavior is described by a nonlinear backbone curve along with rules for constructing unloading and reloading rules (e.g. Masing's rules). We review the parameters describing the backbone curve and provide guidelines for evaluating those parameters given the information typically available from geotechnical site investigations. Issues related to the simultaneous matching of modulus reduction and damping curves are also discussed.
4. Using available vertical array data, nonlinear codes are applied using recorded downhole motions along with the code usage protocols from (1)-(3). We evaluate residuals between recorded and calculated ground surface motions to assess the codes' performance.
5. The results from (4), along with additional simulations run at stronger levels of shaking, are compared to similar results from equivalent-linear analysis to investigate differences between results provided by the two methods of analysis.

Issues (1)-(2) are presented in detail by Kwok et al. (2007) and hence are discussed here only briefly.

NONLINEAR TIME DOMAIN METHODS OF ANALYSIS

Equivalent-linear methods of analysis, which operate in the frequency domain, use for each layer of the site time-invariant soil properties (shear modulus G and soil hysteretic damping β). Time-domain analysis methods allow soil properties within a given layer to change with time as the strains in that layer change. Modified frequency-domain methods have also been developed (Kausel and Assimaki, 2002; Assimaki and Kausel, 2002) in which soil properties in individual layers are adjusted on a frequency-to-frequency basis to account for the strong variation of shear strain amplitude with frequency. Since the frequencies present in a ground motion record vary with time, this can provide a reasonable approximation of the results that would be obtained from a truly nonlinear, time-stepping procedure. Nonetheless, the present focus is on true, time-stepping procedures.

The method of analysis employed in time-stepping procedures can in some respects be compared to the analysis of a structural response to input ground motion (Clough and Penzien, 1993; Chopra, 2000). As shown in Figure 1, the layered soil column is idealized either as a multiple degree of freedom lumped mass system or a continuum discretized into finite elements with distributed mass. Whereas frequency-domain methods are derived from the solution of the wave equation with specified boundary conditions, time domain methods solve a system of coupled equations that are assembled from the equation of motion. Table 1 summarizes the manner in which mass is distributed and nonlinear behavior is simulated for the five nonlinear codes considered here.

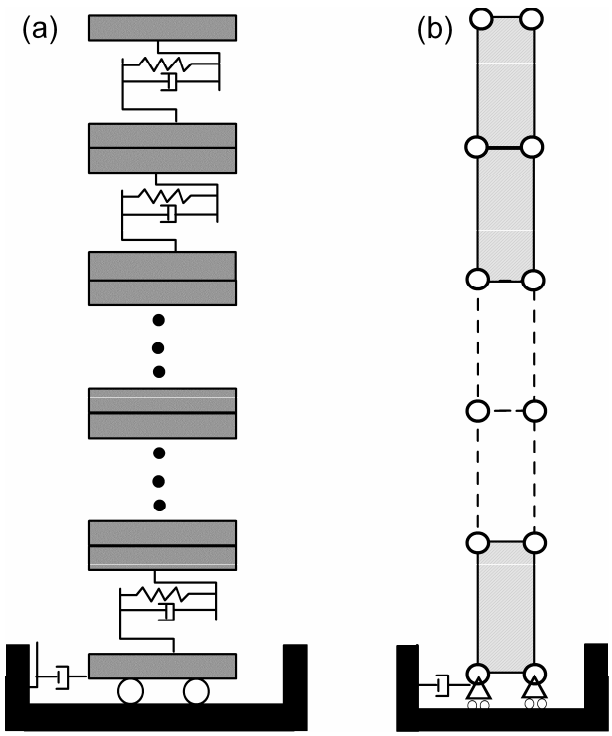

FIG. 1. (a) lumped mass system; (b) distributed mass system

The system of coupled equations is discretized temporally and a time-stepping scheme such as the Newmark β method is employed to solve the system of equations and to obtain the response at each time step. TESS utilizes an explicit finite difference solution of the wave propagation problem that is the same as the solution scheme used in FLAC developed by HCItasca. Unlike in frequency-domain analysis where the control motion could be specified anywhere within the soil column, in time domain analysis the control motion must be specified at the bottom of the system of lumped masses or finite elements.

Table 1. Mass representation and constitutive models used in nonlinear codes

Nonlinear Code	Mass Representation	Constitutive Model
D-MOD_2	Lumped Mass	MKZ (Matasovic and Vucetic , 1993)
DEEPSOIL	Lumped Mass	Extended MKZ (Hashash and Park, 2001)
OpenSees	Distributed Mass	Multi-yield surface plasticity (Ragheb, 1994; Parra, 1996; Yang, 2000)
SUMDES	Distributed Mass	Bounding surface plasticity (Wang, 1990) and other models
TESS	Distributed Mass	HDCP (EPRI, 1993)

NONLINEAR CODE USAGE AND PARAMETER SELECTION PROTOCOLS

Specification of Input Motion

Input motions are specified at the bottom of the 1D site profile in nonlinear analyses. There has been confusion regarding whether the motions specified at the base of the profile should represent an outcropping condition (i.e., equivalent free-surface motions that are twice the amplitude of the incident wave due to full reflection) or a within condition (i.e., the sum of the incident waves and downward propagating waves reflected from overlying layer interfaces). A closely related question is whether the base condition (representing the material below the site column) should be elastic or rigid. For some of the codes used in this research, past practice had been to calculate within motions at the profile base using equivalent-linear analyses, and specify those motions as the input for nonlinear analysis along with an elastic base. For other codes, full outcropping motions were used with an elastic base.

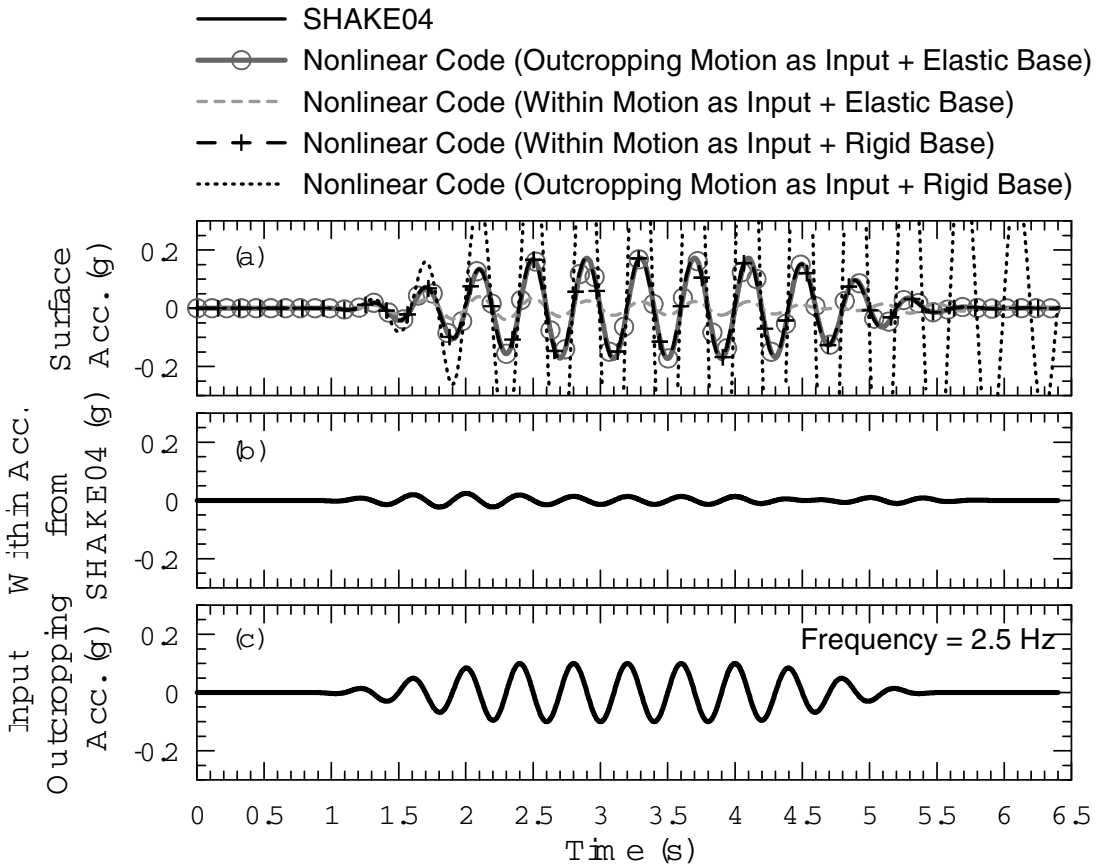

FIG. 2. Acceleration histories for the one-layer problem (Kwok et al. 2007)

To clarify this issue, we exercised nonlinear codes for cases with known elastic solutions. An illustrative example of those calculations is a single soil layer (thickness = 30 m; V_s = 300 m/s) overlying an elastic half-space with V_s = 600 m/s. All soil properties were taken as elastic, and viscous damping was set to zero (i.e., the nonlinear codes

were used with linear backbone curves). A sinusoidal acceleration history matching the site frequency of 2.5 Hz was specified at the top of the halfspace for time domain analyses. The same motion was specified as outcropping for linear frequency domain analyses (SHAKE04, Youngs, 2004).

Figure 2 (bottom frame) shows the input acceleration history, while the middle frame shows the resulting within motion at the layer interface from frequency-domain analyses. Since the 2.5 Hz motion has a node (i.e., zero amplitude at all times) at the interface depth, the within motion decays to null upon achieving a steady state condition. As shown in Figure 2 (top frame), surface acceleration histories obtained from both frequency and time domain analyses match well. These and other similar results suggest that input motions should be specified for an outcropping condition in time domain analyses, and used with an elastic base. Other work has similarly shown that within motions can be used with a rigid base, which would be appropriate practice for applying recorded downhole motions in time domain analyses (Kwok et al., 2007).

Specification of Viscous Damping

In most nonlinear codes, some form of viscous damping is used to provide for damping in the analysis at very small strains where the hysteretic damping from the non-linear soil models is nearly zero (an exception is TESS, which does not require viscous damping). There are a number of options for modeling viscous damping. As illustrated in Figure 3, there are three principal issues: (1) the form of the damping formulation (simplified versus full or extended Rayleigh damping; Park and Hashash, 2004); (2) the target viscous damping ratio (labeled ζ_{tar} in Figure 3) that is matched at specified target frequencies; and (3) the matching frequencies (one, two, and four for simplified, full, and extended Rayleigh damping, respectively). The current versions of all the aforementioned codes except TESS allow use of simplified and full Rayleigh damping. Extended Rayleigh damping is available in DEEPSOIL. TESS does not use Rayleigh damping, instead utilizing unload-reload rules that provide hysteretic damping even at small strains.

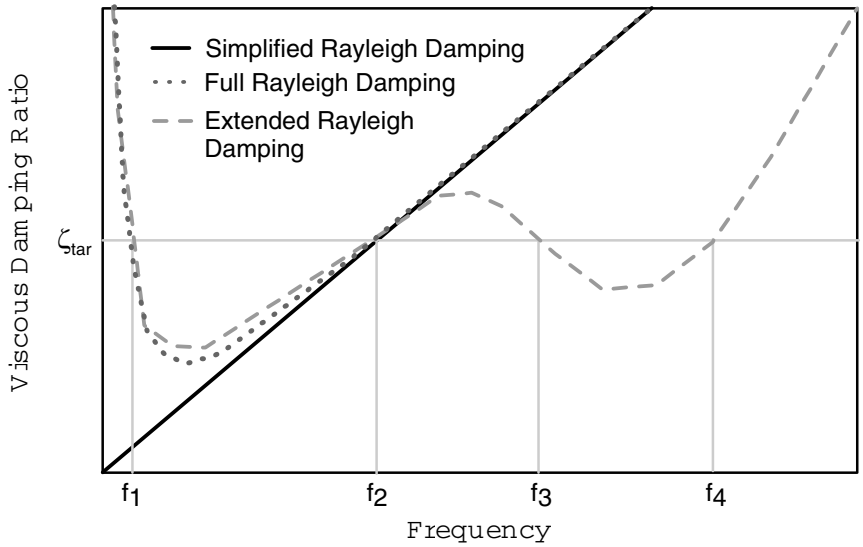

FIG. 3. Illustration of viscous damping models (after Park and Hashash, 2004)

Few protocols are available for guiding users in the selection of the model-type and parameters described above. One set of guidelines has been presented by Park and Hashash (2004) in which the model parameters are selected through an iterative process in which frequency and time domain elastic solutions are matched over a frequency range of interest (because frequency domain analyses using equivalent viscous damping provide a "correct" response against which the viscous damping formulation for the time domain can be calibrated). The procedure is implemented through a user interface.

Kwok et al. (2007) compared results of linear time domain analyses for three site profiles to solutions from linear frequency domain analyses with a specified amount of equivalent viscous damping (fixed at 5%). The three selected sites represent a broad range of site conditions: shallow stiff soil over rock, soft clay overlying stiffer sediments and rock, and very deep soils typical of the Los Angeles basin. A representative example of these results is shown in Figure 4 for a deep soil site (La Cienega). In Figure 4, the red spectrum (equivalent linear) represents the "correct" result to which the time domain results are compared. Equivalent-linear analyses are exact in this case because the analyses are linear visco-elastic.

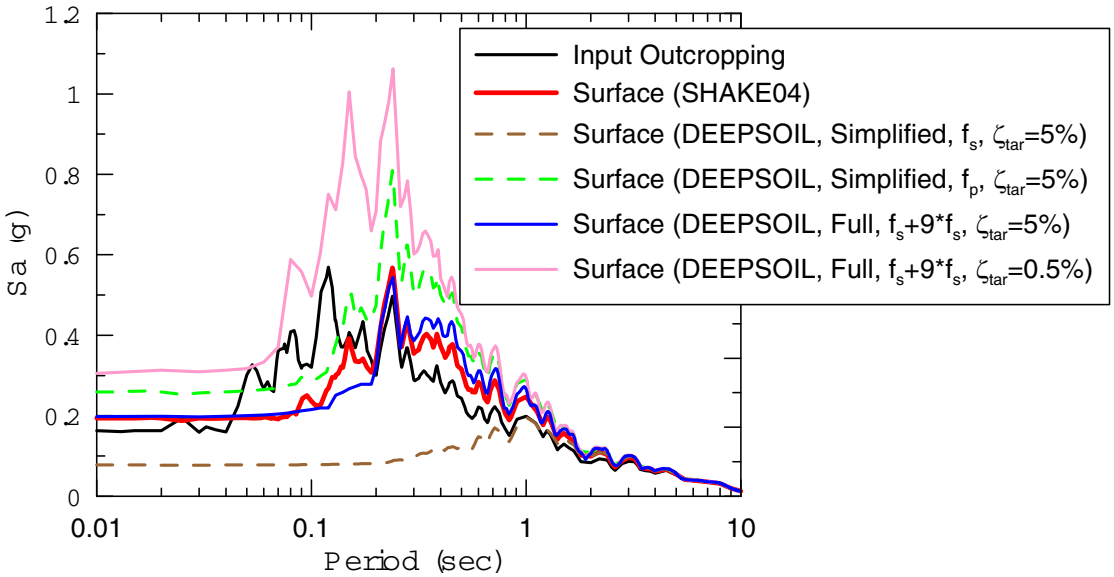

FIG. 4. Comparison of response spectra for La Cienega. Results are shown for DEEPSOIL, but similar results were obtained for D-MOD_2 and OPENSEES.

The principal results of these simulations, most of which are illustrated in Figure 4, are as follows:

- Full Rayleigh damping is preferred to simplified. Figure 4 shows examples of significant misfit in the simplified Rayleigh damping results – a low matching frequency (f_s=site frequency) produces overdamping while a high matching frequency (f_p=predominant frequency of input motion) produces underdamping. The point is that a good match over a wide frequency range is generally not possible with a simplified Rayleigh damping model. The full Rayleigh damping result in Figure 4 (blue line) is based on matching frequencies iterated on to

optimize the fit per the Park and Hashash (2004) procedure; it is seen that the second matching frequency is able to significantly improve the fit.

- The target damping level should match the small-strain soil damping (5% in Figure 4). The use of a much smaller damping value has been advocated by some users. As shown in Figure 4 (result for 0.5%, pink spectrum) produces underdamping.
- For applications where a non-iterative procedure is desired for specification of full Rayleigh damping target frequencies, the site frequency and five times the site frequency will usually suffice (not illustrated in Figure 4).

Parameterization of Nonlinear Material Behavior

Backbone Curve

Figure 5 shows a typical nonlinear backbone curve for a soil element, which has a hyperbolic shape defined by initial small strain secant shear modulus (G_{max}) and shear strength (τ_{ff}). The classical definition of reference strain is the ratio $\gamma_{ref} = \tau_{ff} / G_{max}$ (Hardin and Drnevich, 1972). The parametric description of the nonlinear backbone curve in the past has generally required the specification of this reference strain along with a number of curve fitting parameters. A practical problem with this approach is that the shear strength at rapid strain rate, needed to define reference strain, is often not available. Another problem is that the shape of the backbone curve at small strains may be inconsistent with laboratory test data.

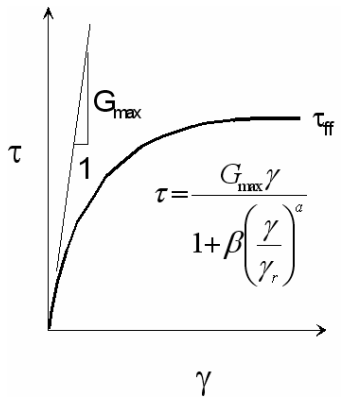

FIG. 5. Schematic illustration of backbone curve used for nonlinear ground response

At least for problems involving low to moderate strain levels, a "pseudo-reference strain" (γ_r) can be used in lieu of the strength-based reference strain. The term pseudo-reference strain is used to avoid confusion with reference strain as defined by Hardin and Drnevich (1972). Pseudo reference strain is defined from a laboratory modulus reduction curve as the shear strain at which $G/G_{max} = 0.5$. This definition arises from hyperbolic fits of G/G_{max} curves according to

$$G / G_{\max} = \frac{1}{1 + \beta\left(\gamma / \gamma_r\right)^a} \tag{1}$$

where β and a are fitting parameters generally taken as 1 and 0.92, respectively (Darendeli, 2001). The advantages of using pseudo reference strain are that (1) γ_r can be readily evaluated from material-specific modulus reduction curves evaluated from laboratory testing and (2) lacking material-specific testing, empirical relationships exist to predict γ_r as a function of basic parameters such as PI, overburden stress, and overconsolidation ratio (Darendeli, 2001; Zhang et al., 2005).

Because pseudo reference strains are determined from modulus reduction curves that are typically defined for strains less than 1%, a backbone curve described by a hyperbolic curve fit using γ_r would not necessarily be expected to accurately represent soil behavior at large strain, including the shear strength. We investigate this problem by examining the degree to which the shear strength implied by the use of Eq. 1 (approximately $G_{max} \times \gamma_r$) is realistic. This is done using ratios of G_{max} to shear strength, for which empirical relationships are available from Weiler (1988). The ratios from Weiler are for soils with OCR=1-5, confining pressures σ= 100-500 kPa and PI=15-45. Weiler's undrained shear strengths (S_u) are based on direct simple shear testing. Weiler's G_{max} / S_u ratio is compared to the inverse of Darendeli's (2001) estimate of γ_r (which is approximately the ratio of G_{max} to the large-strain asymptote of the hyperbolic curve, taken as shear strength).

As observed from Figure 6, the G_{max}/effective-strength ratios implied by pseudo reference strain γ_r are significantly higher than those from Weiler for an overburden stress of σ =100 kPa. This bias implies that the shear strength implied by γ_r is underestimated by Darendeli's relationships at σ=100 kPa. This bias disappears at larger overburden pressures (σ=500 kPa). Accordingly, at relatively shallow depths, the use of backbone curves derived from the pseudo reference strain parameter may overestimate the soil nonlinearity at large strains.

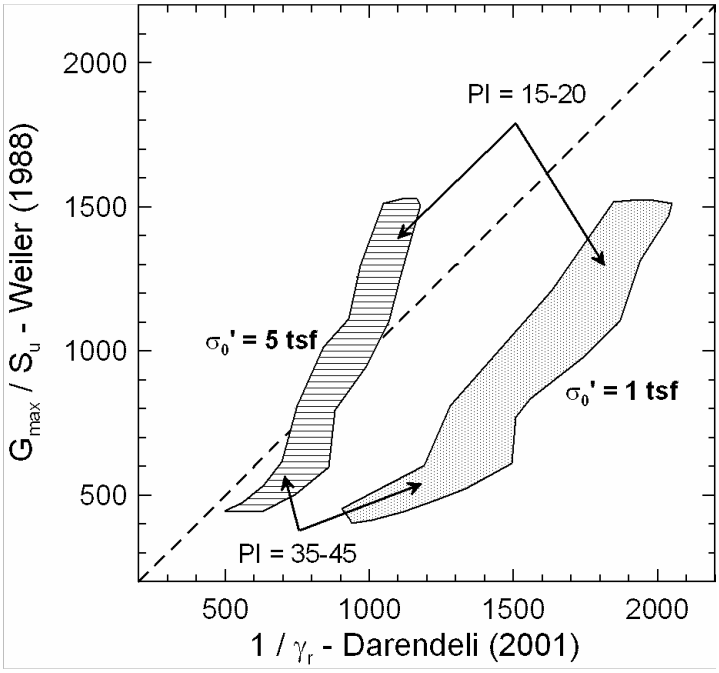

FIG. 6. Comparison of G_{max}/S_u ratio from Weiler (1988) to inverse of pseudo reference strain ($1/\gamma_r$) from Darendeli (2001). Quantity $1/\gamma_r$ is approximately the ratio of G_{max} to the shear strength implied by the use of pseudo reference strain for fitting nonlinear backbone curves.

Recommendations for the evaluation of backbone curve parameters are given in a subsequent section following a discussion of material damping.

Material Damping

Masing's rules (Masing, 1926) and extended Masing rules (Vucetic, 1990; Pyke, 1979) are employed in nonlinear analysis in conjunction with the backbone curve to describe unloading, reloading and cyclic degradation behavior of soil. Material damping is directly proportional to the area contained within a cyclic stress-strain loop, and hence is sensitive to the shape of the backbone curve and unload/reload rules. The damping at large strain that results from the use of Masing or extended Masing rules tends to be over-estimated relative to laboratory measurements.

There are three schools of thought on managing the over-estimation of damping. One approach is to select model parameters for the backbone curve (and hence modulus reduction curves) that optimally fit the target data and accept the resulting overestimation of damping using Masing's rules. A second approach is to select model parameters that optimize the fitting of modulus reduction and damping curves simultaneously (across the strain range of interest).

The third approach is to introduce an additional parameter that changes the shape of the unload/reload curves so that both modulus reduction and damping curves can be fit simultaneously. Lo Presti et al. (2006) allows unloading and reloading curves to have a shape scaled from that of the backbone curve by a factor of n (for the original Masing criteria, $n = 2$). Lo Presti et al. provide recommendations for estimating n as a function of soil type, strain level and number of cycles for the motion. Wang et al. (1980) suggest an approach in which a damping correction factor is applied to the Masing rule damping. These unload/reload rules are not yet implemented in the nonlinear codes listed in Table 1, and hence this approach is not discussed further.

Parameter Selection for Backbone Curves and Damping

There are two basic elements to the specification of parameters describing the nonlinear backbone curve and damping. The first element is to select the target shape of the backbone curve (equivalently, the modulus reduction curve) and the damping curve. The second element is to select model parameters that describe the target relationships within a reasonable degree of approximation for the problem at hand.

Element (1) – Target Curves: The ideal characterization would involve material-specific cyclic testing across the strain range of interest. This testing would include characterization of the material's dynamic shear strength for large-strain problems. However, material specific testing is usually not available, requiring the nonlinear behavior to be described using published correlations relating soil index properties, stress state, and stress history to parameters describing modulus reduction and damping curves (e.g., Darendeli, 2001; Zhang et al., 2005). Those relationships are usually well defined to shear strains of approximately 0.3-0.7%. This is illustrated in Figure 7, which shows the modulus reduction-strain values in the database used by Darendeli (2001). As described previously, those relationships do not typically provide an adequate representation of the shear strength. Guidelines for undrained shear strength evaluation and estimation are given in Ladd (1991); those estimates should be adjusted in consideration of rate effects, as described for example by Sheahan et al. (1996).

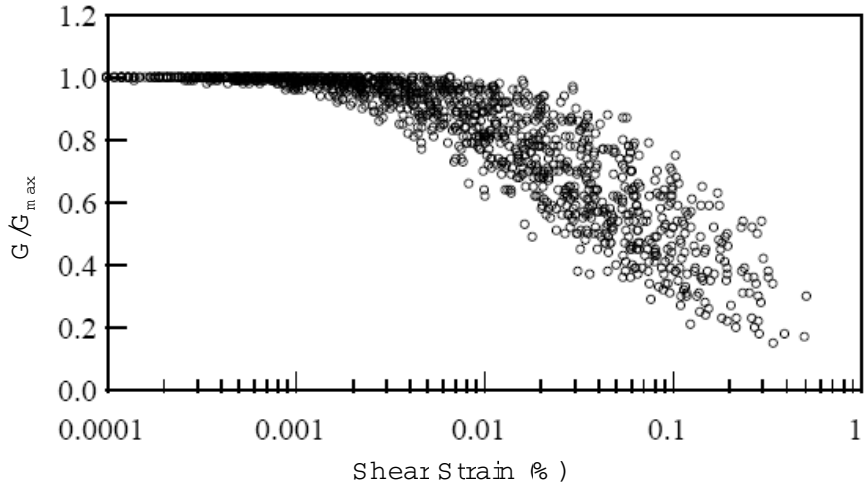

FIG. 7. Modulus-reduction-strain values in the database used by Darendeli (2001)

For problems involving large strain soil response, traditional practice has been to use a hyperbolic stress-strain curve (Eq. 1) with the strength-based reference strain. However, as shown in Figure 8, because of the misfit of reference strain and pseudo reference strain, this approach provides a poor match to small-strain modulus reduction behavior from laboratory tests. Accordingly, we recommend an alternative approach illustrated in Figure 8 and explained in the following: (1) use cyclic test results or correlation relationships to define the shape of the backbone curve to strain level γ_1 (typically taken as 0.1-0.3%); (2) estimate the material shear strength (τ_{ff}) for simple shear conditions with appropriate adjustment for rate effects; (3) estimate modulus reduction ordinates between strain γ_1 and the shear strength with the following hyperbolic relationship:

$$G / G_{\gamma_1} = \frac{1}{1 + G_{\gamma_1}(\gamma - \gamma_1)/\tau_{ff}} \quad \text{(applies for } \gamma > \gamma_1 \text{ only)} \qquad (2)$$

where $G_{\gamma 1}$=secant shear modulus from Step (1) at $\gamma=\gamma_1$. An example application of this procedure is given by Chiu et al. (2008). At present, only OpenSees allows the input of the G/G_{max} curve ordinates so that this formulation could be directly applied.

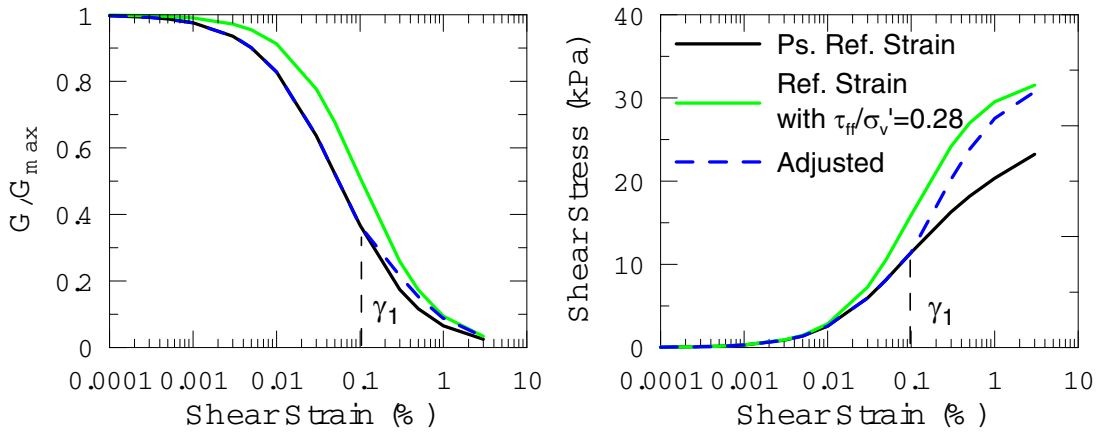

FIG. 8. Modulus reduction and stress-strain curves implied by pseudo reference strain from Darendeli (2001), reference strain model, and proposed procedure (*PI*=20, *OCR*=1, σ_v'= 100 kPa, V_s=135 m/s)

Element (2) – Approximation of Target Curves: As noted above, an exact match of target curves is not possible when Masing rules or extended Masing rules are used to describe the unload-reload relationship. Until nonlinear codes implement the capability to simultaneously match both modulus reduction and damping curves, mis-match of one or both of these curves is unavoidable. As mentioned previously, one approach is to match the target modulus reduction curve as accurately as possible and accept the misfit of damping. Another is to optimize the fit of both simultaneously.

We have worked with Hashash and Phillips (pers. comm., 2006) to devise a scheme to search for model parameters to achieve the aforementioned fitting approaches (in addition, the scheme allows optimization of the fitting of the damping curve only, although this approach is usually not considered). The scheme requires the specification of target material curves at (user-) predetermined strain levels. The fitting error is considered up to a maximum strain level (usually between 0.1 and 1%). The best combination of model parameters would be the one that gives the least error between the target curves and model curves. This error is quantified as:

$$\varepsilon = \sqrt{(w_{G/G_{\max}} \times \bar{\varepsilon}_{G/G_{\max}})^2 + (w_\beta \times \bar{\varepsilon}_\beta)^2} \tag{3}$$

where $\bar{\varepsilon}_{G/G_{\max}}$ and $\bar{\varepsilon}_\beta$ represent the mean error for the fitting of modulus reduction and damping curves respectively. Error term $\bar{\varepsilon}_{G/G_{\max}}$ is calculated as:

$$\bar{\varepsilon}_{G/G_{\max}} = \frac{\sqrt{\sum \left(\varepsilon_{G/G_{\max}}(\gamma_i)\right)^2}}{N} \tag{4}$$

The numerator in Eq. 4 is the summation of fitting error from the lowest specified strain level to the maximum strain level. N is the number of strain levels included in the summation. Error term $\bar{\varepsilon}_\beta$ is calculated in a similar way as for $\bar{\varepsilon}_{G/G_{\max}}$. Terms $w_{G/G_{\max}}$ and w_β in Eq. 3 are weight factors whose values depend on the choice of fitting approach. Table 2 summarizes the values of weight factors under different fitting approaches. Figure 9 shows the difference in the fitted modulus reduction and damping curves (relative to target data) when different fitting approaches are employed.

Table 2. Weight criterion for different fitting approaches

Fitting Approach	Weight Criterion
MR	$w_{G/G_{\max}} = 1;\ w_\beta = 0$
MRD	$(w_{G/G_{\max}})^2 + (w_\beta)^2 = 1$ $\frac{w_{G/G_{\max}}}{w_\beta} = \begin{cases} 1, & \beta_{\max} > 25\% \\ 1 + \frac{0.25 - \beta_{\max}}{0.15}, & 10\% < \beta_{\max} < 25\% \\ 2, & \beta_{\max} < 10\% \end{cases}$
D	$w_{G/G_{\max}} = 0;\ w_\beta = 1$

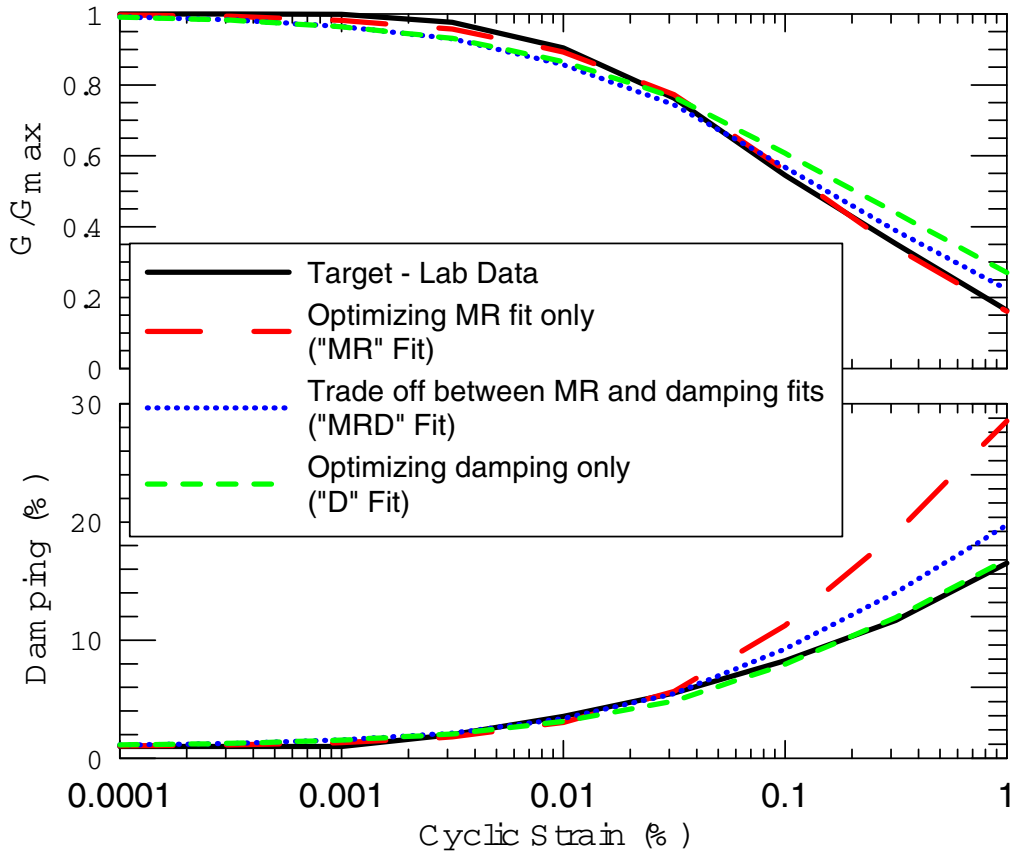

FIG. 9. Different approaches in fitting modulus reduction and damping curves in nonlinear analysis

To illustrate how different fitting approaches may influence ground motion predictions, nonlinear ground response analyses are performed for two strong motion sites with different fitting of target curves. The two sites are Apeel 2 in Redwood City, which is a soft clay site consisting of Bay Mud, and Sepulveda VA hospital in Los Angeles, which is a relatively stiff soil site. The calculations were performed using the DEEPSOIL code. The target nonlinear modulus reduction and damping curves were taken as Seed and Idriss (1970) upper bound for modulus reduction and lower bound for damping in shallow sand layers, EPRI (1993) deep curves (251-500 ft) for deep sand (depth > 60 m), Sun et al. (1988) for Bay Mud at Apeel 2, and Vucetic and Dobry (1991) for other clayey soils. Scaled versions of an outcropping broadband synthetic motion (Silva, pers. comm., 2004) are used as input. Figure 10 shows predicted ground surface motions for Apeel 2 and Sepulveda, respectively. It is observed that when the input motion is relatively low-amplitude (about 0.2 g), predictions for all three fitting approaches are similar. When the shaking is relatively strong (about 0.7 g), predictions for the "MR" fitting approach are smaller than those from the other approaches, which is due to the larger high-strain damping ratio associated with the "MR" fitting approach. Another observation is that the soft site is more sensitive to the different fitting approaches than the stiff site. This occurs because the softer site has larger strains for a given input motion amplitude.

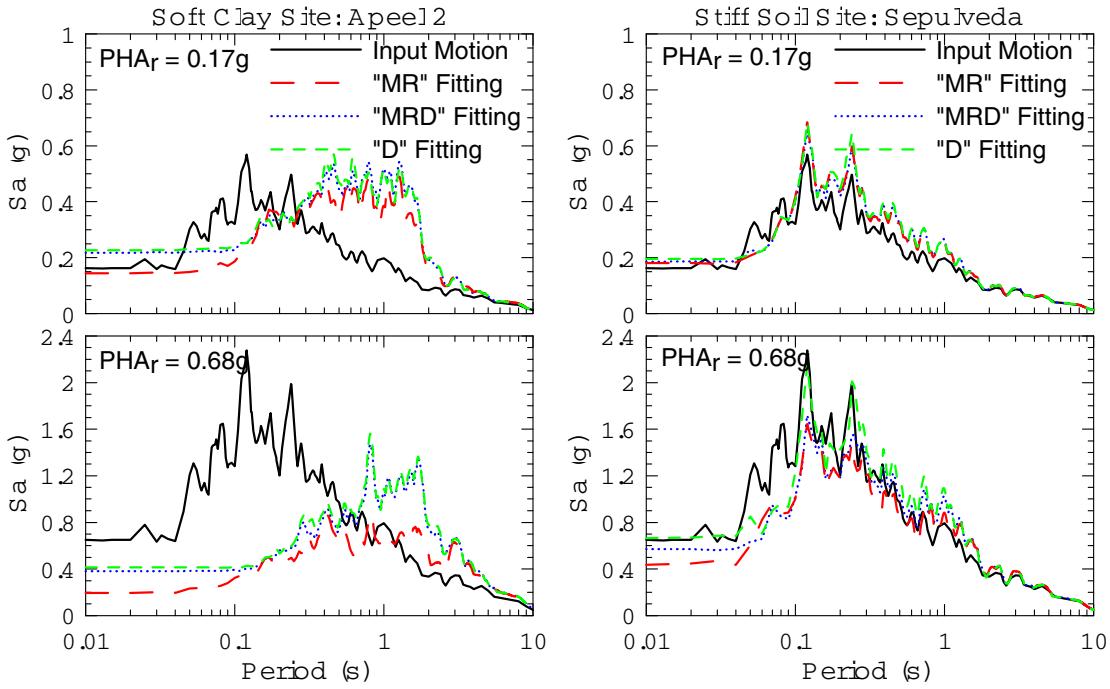

FIG. 10. Prediction results for soft clay site (Apeel 2) and stiff soil site (Sepulveda) with model curves obtained from different approaches to fitting modulus reduction and damping curves in nonlinear analysis

VALIDATION OF CODE PREDICTIONS AGAINST VERTICAL ARRAY DATA

Having developed the parameter selection protocols, it is necessary to test the effectiveness of those protocols by comparing code predictions to data. It is also important to study the uncertainties in predictions due to various sources of variability (material properties and modeling schemes). We utilize data from vertical array sites for this purpose. Four vertical array sites have been considered to date: Turkey Flat, California; La Cienega, California; KGWH02, Japan (Kiknet site); and Lotung, Taiwan. Analyses are preformed using an equivalent-linear procedure (SHAKE04) and the nonlinear codes listed in Table 1.

We describe the results for the La Cienega site in some detail. Brief overviews of the principal findings from the other sites are then provided.

La Cienega Site

Site Model and Strong Motion Data

We define "baseline" dynamic properties for the site along with a representation of material property variability. The baseline shear wave velocity (V_s) profile was developed from site-specific SASW and suspension logging data. Baseline modulus reduction and damping curves are derived from material-specific testing for 13 depth intervals. Log-normal, depth-dependent standard deviations on V_s are taken from an

empirical model (Toro, 1997). Log-normal standard deviations on modulus reduction and damping curves are taken as the standard deviations of the Darendeli (2001) model residuals. Additional details on the selected soil properties are given in Stewart et al. (2007). Strong motion data are taken from a M_w=4.2 event that occurred 2.7 km from the site on 09/09/2001.

Comparison of Model Predictions to Data

Figure 11 shows 5% damped acceleration response spectra of the horizontal recorded surface motions and prediction results obtained using the baseline geotechnical model while Figure 12 compares the predicted acceleration histories with the recordings (DEEPSOIL predictions only). Residuals are calculated as:

$$R(T) = \ln\left(S_a(T)\right)_{data} - \ln\left(S_a(T)\right)_{pre} \quad (5)$$

where $\ln\left(S_a(T)\right)_{data}$ is the natural log of the recording's spectral acceleration at period T and $\ln\left(S_a(T)\right)_{pre}$ is the natural log of the predicted spectral acceleration.

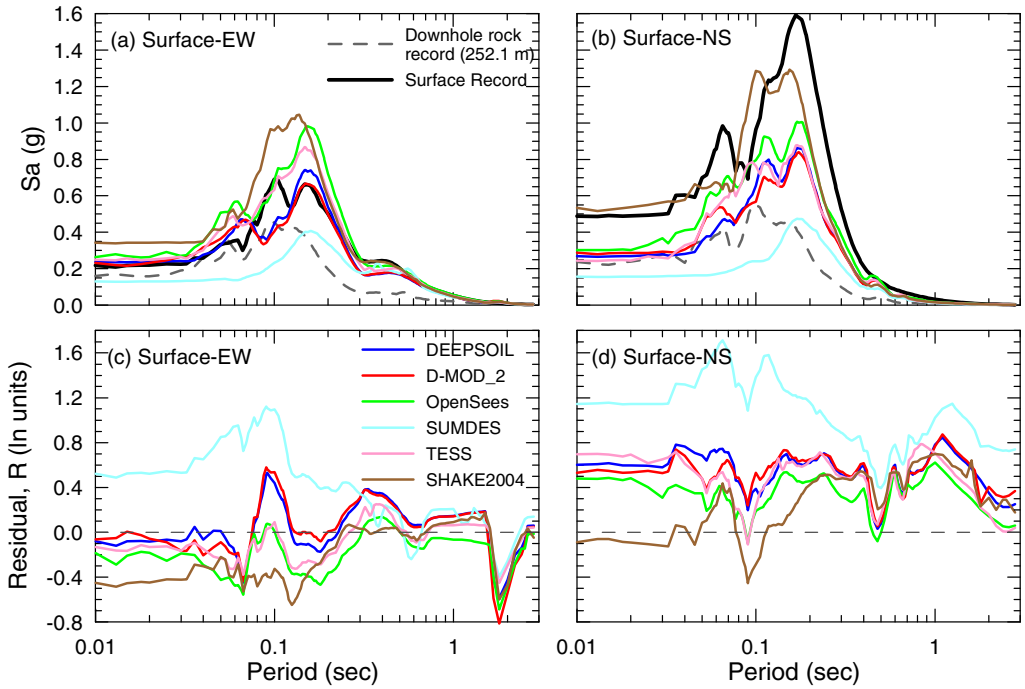

FIG. 11. Acceleration response spectra for data and simulation results compared through direct spectral ordinates and prediction residuals for ground surface. Results shown for two horizontal directions. Results shown to a maximum period of 1/(1.25´f_{HP}), where f_{HP} = high pass corner frequency.

As shown in Figure 12, the general comparison of the acceleration histories to data is quite favorable, although there is some bias towards over-prediction of the largest pulses in the record in the EW direction and under-prediction in the NS direction. The error appears to be related to the shape of the pulses near their tips.

Those errors in the acceleration histories translate into errors in spectra as well. For the

EW component at the ground surface, predictions from codes DEEPSOIL and D-MOD_2 are similar to each other and are generally close to the data, although they are underpredicting at periods between 0.07 and 0.12 sec. Predictions from codes OpenSees and TESS have similar trends and are also close to the data, except for overprediction near the period of 0.15 sec. SUMDES is underpredicting at periods below 0.5 sec which is probably due to the use of a simplified Rayleigh damping formulation in the version of this code that was used. Close examination of the spectra and residuals reveals that predictions from all codes have bumps near T=2 sec, which corresponds to the elastic period of the site from the base recording to the ground surface. For the NS component at the ground surface, all nonlinear codes are underpredicting at periods below 0.5 sec. Although not shown here for brevity, similar misfits of predictions relative to data occur at depths of 18.3 m and 100.6 m.

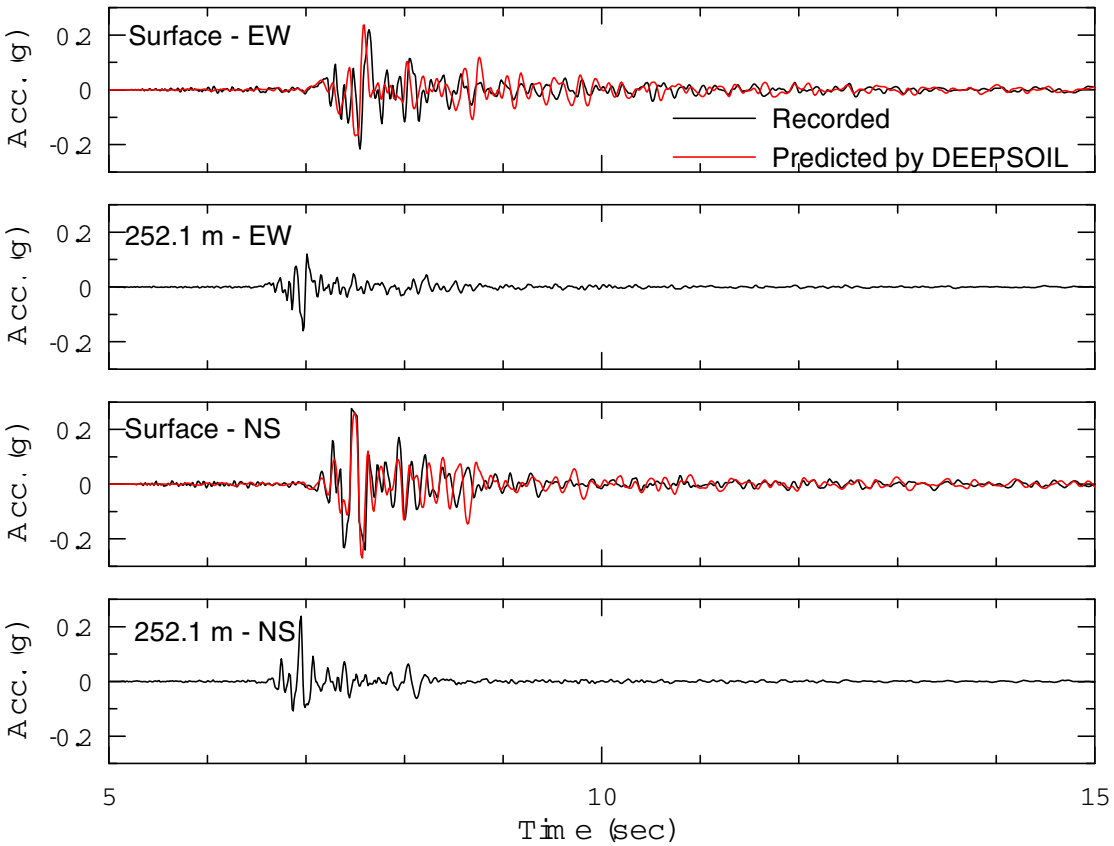

FIG. 12. Acceleration histories for data and simulation results from DEEPSOIL for ground surface

Contributions to the uncertainty in simulation results from model-to-model variability and material variability are considered. To evaluate model-to-model variability, we first take the median estimate $\ln\left(\overline{S}_a(T)\right)$ from the five nonlinear model predictions using baseline properties. Model variability, σ_m, is then calculated from the variance as follows:

$$\sigma_m^2(T) = Var\left(S_a(T)\right)_{pre} = \frac{\sum_i \left[\ln\left(S_a(T)\right)_{pre,i} - \ln\left(\bar{S}_a(T)\right)\right]^2}{N-1} \quad (6)$$

where N = number of predictions (five) and $\ln\left(S_a(T)\right)_{pre,i}$ = natural log of predicted spectral acceleration from code i. Figure 13 shows the variation of σ_m with period.

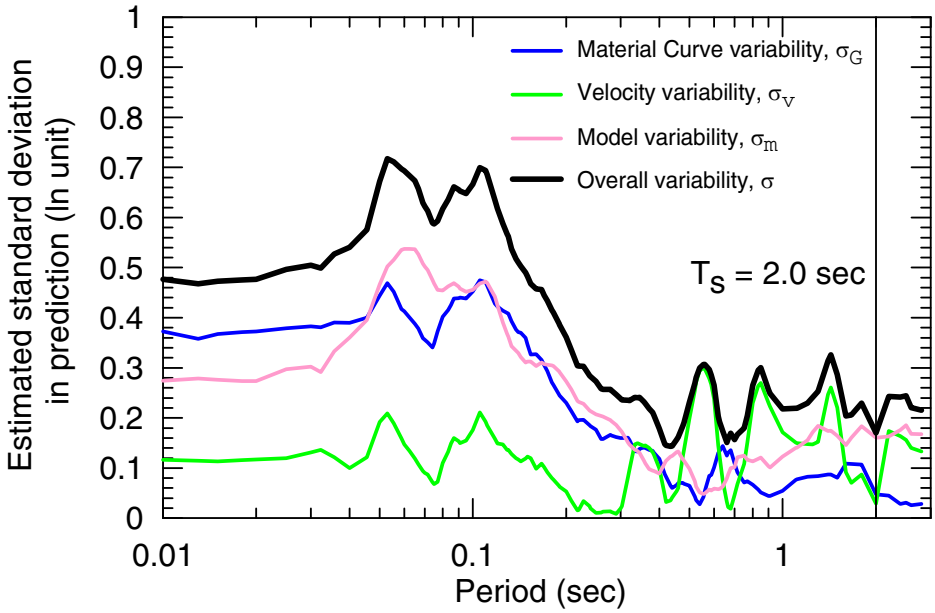

FIG. 13. Standard deviation terms associated with geometric mean acceleration response spectral ordinates for ground surface. T_s = elastic site period.

Variability in predictions from uncertain shear wave velocity and uncertain modulus reduction and damping curves is considered using only the DEEPSOIL code. To calculate the standard deviation due to velocity variability, ground motions are predicted based on two non-baseline velocity profiles (mean ± $\sqrt{3}$ standard deviation velocities). The standard deviation of the ground motions due to the variability in velocity (denoted σ_v) is estimated according to the first-order second moment (FOSM) method (Baker and Cornell, 2003; Melchers, 1999) as follows:

$$\sigma_v = \sum_{i=1}^{3} w_i (\ln(S_a(T)_i - \overline{\ln(S_a(T))})^2 \quad (7)$$

where

$$
\begin{aligned}
&S_a(T)_1 = S_a(T)_{V_s:\mu} \\
&S_a(T)_2 = S_a(T)_{V_s:\mu+\sqrt{3}\sigma_{V_s}} \\
&S_a(T)_3 = S_a(T)_{V_s:\mu-\sqrt{3}\sigma_{V_s}} \\
&\overline{\ln(S_a(T))} = \sum_{i=1}^{3} w_i \ln(S_a(T)_i) \\
&w_1 = 2/3;\ \mathrm{w}_2 = \mathrm{w}_3 = 1/6
\end{aligned}
\tag{8}
$$

The standard deviation due to the variability in material curves (denoted σ_G) is estimated similarly to σ_v. Figure 13 shows the estimated standard deviation in prediction due to different sources of variability. For $T < 0.4$ sec, the model and material curve variability dominate while for $T > 0.4$ sec velocity variability is strongest.

To study site response at different levels of input motion, site amplification factors are compiled from ground motions recorded at La Cienega from 1999-2005. Predicted amplification factors of geometric mean response spectral accelerations are derived at specified periods using the baseline geotechnical model for all codes. To estimate amplification factors for different amplitudes of input motions, the recording shown in Figure 12 is scaled down to various degrees. Figure 14 shows that the predicted amplification factors demonstrate a similar trend with respect to base motion peak acceleration (PGA^r) as those observed from data. This suggests that nonlinearity is modeled well by nonlinear codes over this range of input motions. The level of predicted amplification is biased at multiple periods. For example, at the elastic site period (2 sec), the predicted amplification is larger than suggested by data.

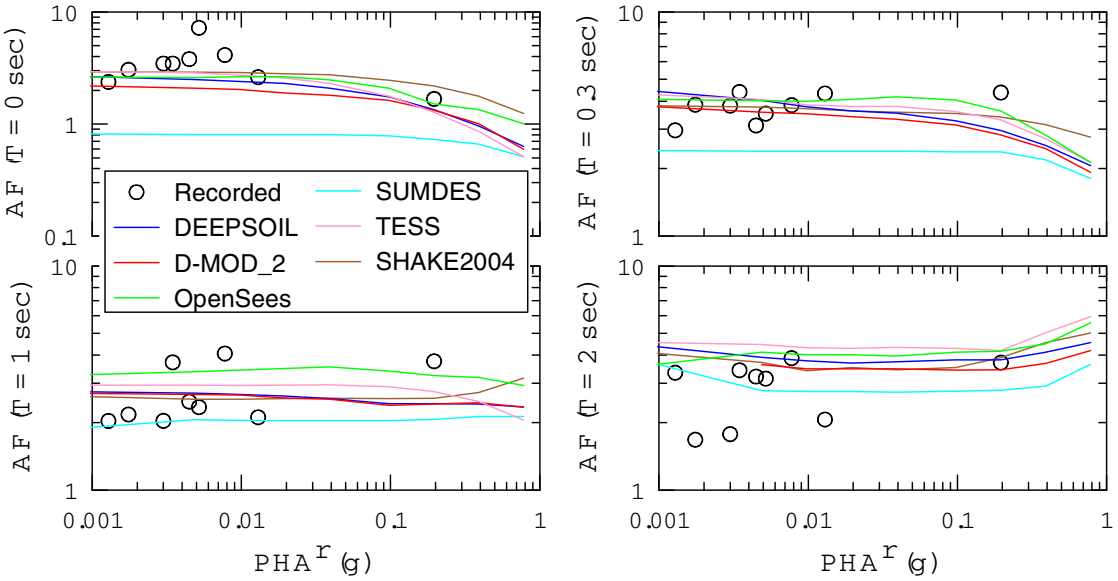

FIG. 14. Theoretical and observed amplification factors at the La Cienega site.

Other Sites

Three other vertical array sites were analyzed in a manner similar to La Cienega – Turkey Flat, KGWH02 (Kiknet), and Lotung. Results for all sites are given in Stewart et al. (2007). Results for the Turkey Flat site, which were originally provided as part of a blind prediction exercise, are also given in Kwok et al. (2008 – in press).

For all sites except Turkey Flat, residuals for very low periods (reflecting PGA) are positive, indicating that the models are underpredicting high frequency components of ground motion. Near the elastic site period (T_s), the models produce a local "bump" in the spectrum that results in overprediction. At periods significantly greater than T_s, residuals disappear due to the lack of a significant site effect.

The above misfits can have many sources. In general, there are two possible sources of misfit – error in the input data (velocity profiles or nonlinear curves) or error in the models and their parameter selection protocols. Errors in velocity profile were checked by comparing observed (small amplitude) shear wave travel time to the time implied the model. With the exception of the Kiknet site, these checks confirm the velocity profile used in the analysis. For Kiknet, observed travel times are less than model travel time, which may be due to waves entering from the side of the relatively narrow basin in which the site is located. Apart from velocity, other possible sources of error include incorrect modeling of material curves (modulus reduction and damping) or the presence of site response physics that cannot be captured by a 1D model. Because modulus reduction effects are likely relatively modest given the low strain levels excited by the subject earthquakes, error in the modeling in modulus reduction is not likely the source of the misfit.

Given that site amplification is under-predicted for all three sites considered across a broad frequency range, a likely source of bias is overdamping in the models. This overdamping could reflect bias in the material damping curves or excessive Rayleigh damping. Further research is needed to resolve these possible sources of bias.

We next discuss trends in the period-dependence of the standard deviation terms. In Figure 15, uncertainties in predictions due to different sources of variability are plotted as a function of period (left frame) and period ratio (right frame; period ratio = T/T_s, where T_s = elastic site period). Variability of predictions due to material curve uncertainty seems to be most pronounced at periods less than 0.5 sec and has no clear association with the site period. Moreover, material curve uncertainty only produces significant response variability for relatively thick site profiles – it is not a significant issue for Turkey Flat, which is a shallow soil site.

The effect of velocity variability can have a strong influence on the predictions near the elastic site period. However, this strong influence is only observed for sites with large impedance contrast (Turkey Flat and KGWH02), which dominates the site response in those cases. This is shown in Figure 15 by a peak in the σ_v term near T/T_s = 1.0. Such a peak does not occur for the Lotung or La Cienega sites, which have a gradual variation of velocity with depth and no pronounced impedance contrast.

Model-to-model variability is most pronounced at low periods, where the differences result principally from different damping formulations. Given the modest ground motions at the investigated sites, it is expected that variations in the viscous damping

formulations are principally driving this variability. As noted previously, predictions from SUMDES, which had only the simplified Rayleigh damping formulation at the time these predictions were made, are much lower than the predictions from codes with full Rayleigh damping formulation. This is a major contributor to the model-to-model variability at low periods.

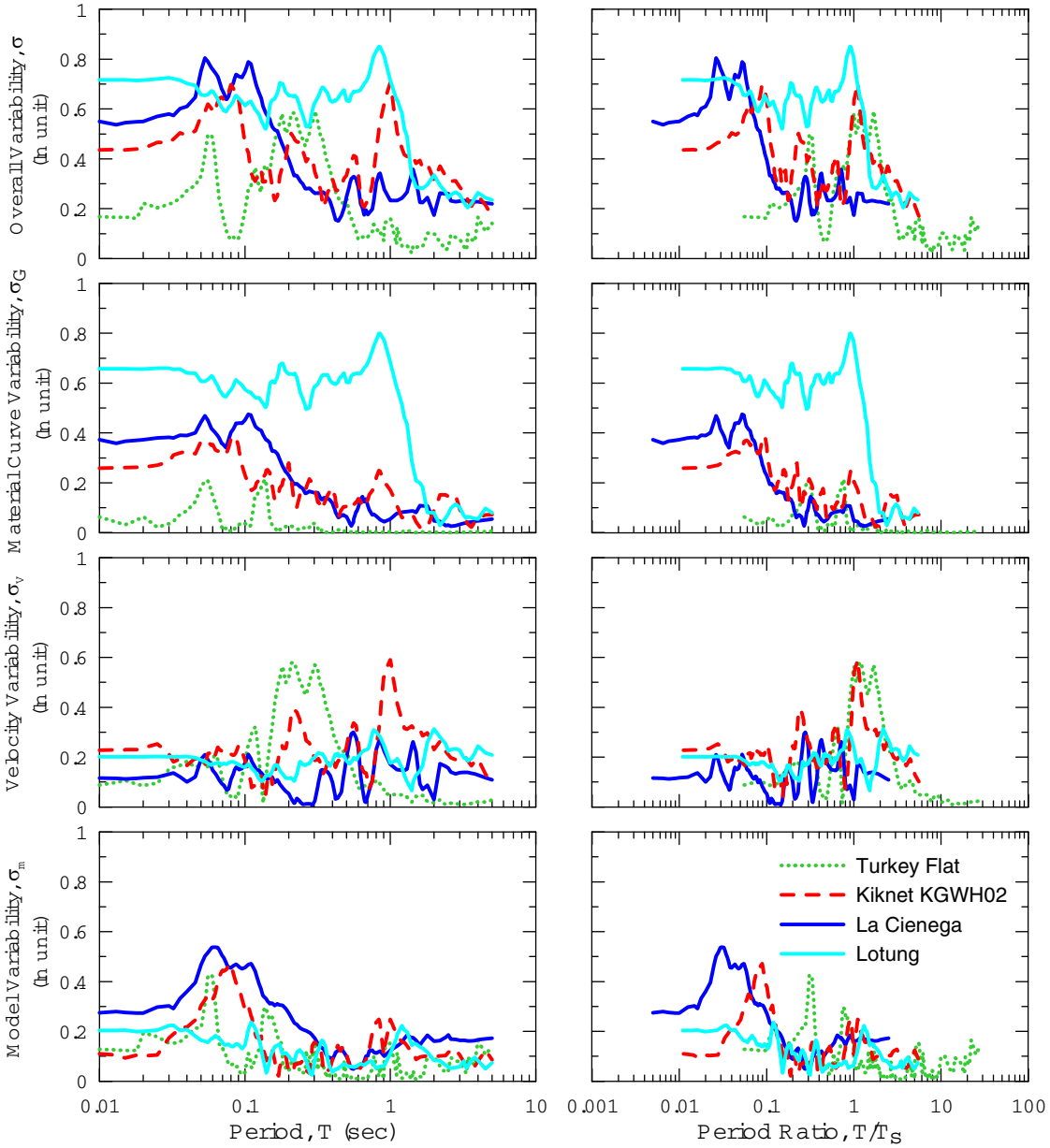

FIG. 15. Comparison of variabilities across four vertical array sites

COMPARISON OF EQUIVALENT LINEAR AND NONLINEAR RESULTS

The predictions of ground motions at vertical array sites described in the previous section were made using both equivalent-linear and nonlinear codes. The aforementioned comparisons of model predictions to data showed similar trends for

both methods of analysis, although the positive residuals at short periods were generally smaller for equivalent-linear.

More meaningful insight into the differences between equivalent-linear and nonlinear ground motion predictions can be made when the codes are exercised at relatively strong shaking levels that induce large strains. Representative results are shown in Figure 16, which shows for the La Cienega site geometric mean horizontal component predicted spectra, amplification factors (=surface/input outcropping spectral accelerations), and spectral shapes (S_a/PGA) for a low-strain condition (left side, which corresponds to observed motions during 2001 event) and a large-strain condition produced through the use of a large amplitude synthetic input motion (right side). The results shown in Figure 16 apply for the baseline geotechnical model described previously. Also shown for reference purposes are predictions of empirical models for amplification (middle frames; Choi and Stewart, 2005) and spectral shape (bottom frames; Campbell and Bozorgnia, 2007). The empirical amplification model is exercised for the site's V_{s30} (260 m/s) and corresponding input *PGA*. The empirical spectrum from which spectral shape is evaluated is calculated using M_w=7.5, site-source distance=10 km, and strike-slip focal mechanism (for synthetic).

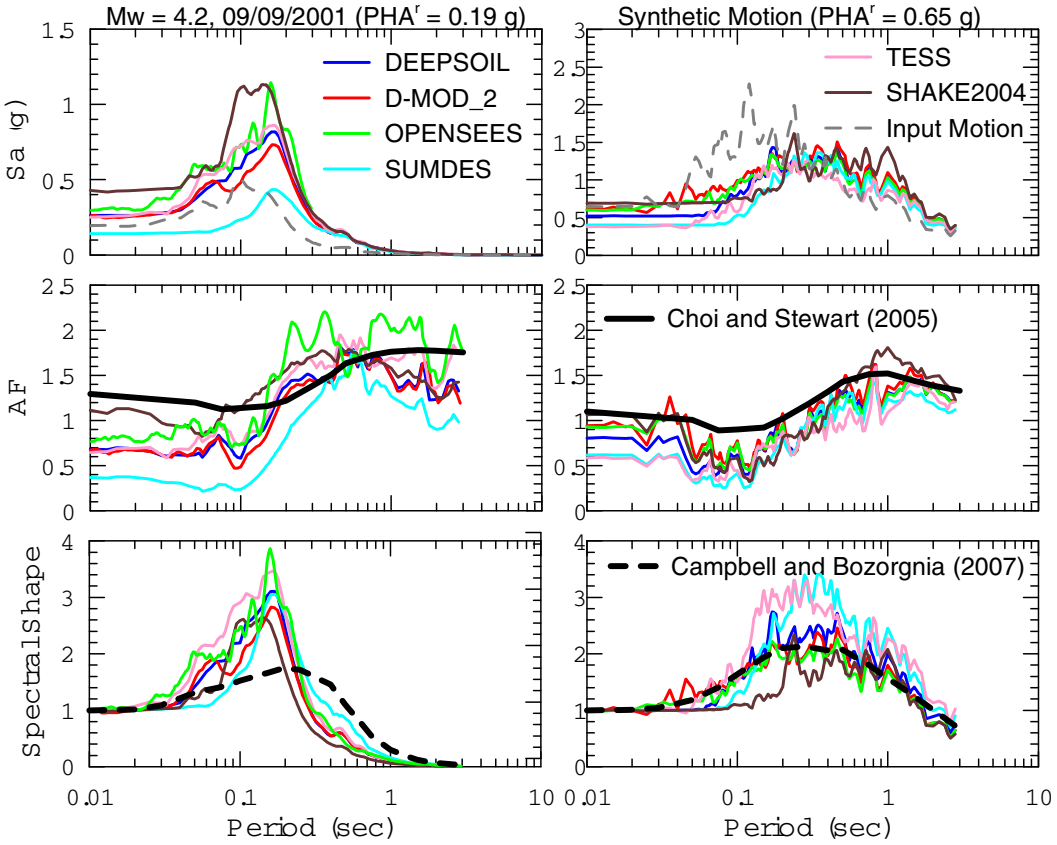

FIG. 16. Comparison of computed spectra, amplification factors, and spectral shapes of predicted motions at La Cienga site

As shown in the bottom frames of Figure 16, the spectral shapes from equivalent-linear and nonlinear models are similar to each other for the 2001 input motion that induces relatively low strain but are significantly different for the large amplitude synthetic

motion. For the large-strain simulation, the spectral shapes at low periods (< ~0.2 sec) from equivalent linear analyses are flatter and have less period-to-period fluctuations than those from nonlinear analyses or empirical models. This aspect of equivalent-linear results is believed to be non-physical and can be overcome with nonlinear analysis. As shown in the middle frames, the flatness of the equivalent linear spectrum is associated with a dip in the amplification factors between periods of approximately 0.03 and 0.3 sec. That dip is less pronounced in the nonlinear codes, which produce amplification factor shapes more compatible with the empirical model.

RECOMMENDATIONS AND CONCLUSIONS

In this article, we present the principal findings of a large, multi-investigatory project directed towards establishing consensus guidelines for the use of nonlinear ground response analyses in engineering practice. Our intent is to make nonlinear analyses more accessible to engineering practitioners and enhance their usage for situations where it is justified. We recognize that the nonlinear codes considered here are one-dimensional, which has its own set of limitations for situations where the site response may be influenced by relatively complex basin geometry or topography.

Nonlinear analyses may provide an improved estimate of ground motion relative to equivalent-linear when ground strains become "large." This can be judged for a given application by examining response spectra and amplification factors from equivalent-linear analysis – caution should be exercised if they exhibit a flat spectrum or a "hole" in the amplification factors at short periods. We speculate that this is caused by overdamping of high-frequency components of ground motion, which occurs principally early in the record (p-waves) when the amplitude of shaking (and material damping) are low. This certainly occurs when shear strains approach 1%, although in deep soil sites it has been observed to occur for peak strains as low as 0.2-0.3%.

When nonlinear analyses are performed, the following guidelines are recommended for code usage and parameter selection:

1. Input motions should be used as-recorded (without modification). Outcropping recorded motions should be applied at the base of a site model with an elastic base. Downhole recorded motions should be applied with a rigid base.
2. For codes that require it, viscous damping should be specified using a full Rayleigh damping formulation with the target damping level ζ_{tar}=small strain soil hysteretic damping. The first matching frequency should be the site frequency. The second frequency should be selected so as to optimize the match of elastic frequency- and time-domain analysis for the site. A reasonable approximation for many applications is to take the second frequency as approximately five times the site frequency.
3. The target backbone curve for a site is best determined through material specific cyclic testing along with dynamic strength testing. If this is not available, the shape of the backbone curve at small- to modest-strains (up to approximately 0.1-0.3%) can be estimated using empirical relationships that take index properties, confining pressure, and stress history as input. Procedures to estimate undrained shear strength through stress

normalization are well established (Ladd, 1991), but require modification for rate effects (e.g., Sheahan et al., 1996).

4. For problems involving small-strain response, target backbone curves can be defined using modulus reduction relationships without consideration of shear strength. For problems involving moderate to large strain response, a hybrid representation that accounts for the shape of the modulus reduction curve at small strains and shear strength at large strain is recommended (see Eq. 2 and Figure 8).
5. Ultimately it is hoped that procedures for simultaneously matching target modulus reduction and material damping curves will be implemented in nonlinear codes, but this is not currently available. At present, users can choose to match the modulus reduction curve only (MR fitting) or modulus reduction and damping curves simultaneously (MRD fitting). We recommend the use of both approaches for large strain problems to bound the solution.

When applied to vertical array sites, these protocols generally produce reasonable results, although there is some indication of possible overdamping at high frequencies and overestimation of site amplification at the resonant frequency of the site model. Additional work to validate and further refine these procedures is ongoing by the project team.

ACKNOWLEDGMENTS

Financial support for the benchmarking of nonlinear ground response analysis procedures was provided by PEER Lifelines project 2G02, which is sponsored by the Pacific Earthquake Engineering Research Center's Program of Applied Earthquake Engineering Research of Lifeline Systems. The PEER Lifelines program, in turn, is supposed by the State Energy Resources Conservation and Development Commission and the Pacific Gas and Electric Company. This work made use of Earthquake Engineering Research Centers Shared Facilities supported by the National Science Foundation under Award #EEC-9701568. In addition, the support of the California Department of Transportation's PEARL program is acknowledged. This work would not have been possible without close collaboration with a number of code developers including Youssef Hashash, Neven Matasovic, Robert Pyke, Zhiliang Wang, and Zhaohio Yang. Their insights and spirit of collaboration are truly appreciated. This project has also benefited from the helpful suggestions of an advisory panel consisting of Drs. Yousef Bozorgnia, Susan Chang, Brian Chiou, Ramin Golesorkhi, I.M. Idriss, Erol Kalkan, Robert Kayen, Steven Kramer, Faiz Makdisi, Geoff Martin, Lelio Mejia, Tom Shantz, Walter Silva, and Joseph Sun. Christine Goulet is thanked for her review of this manuscript.

REFERENCES

Assimaki, D. and E. Kausel (2002). "An equivalent linear algorithm with frequency- and pressure-dependent moduli and damping for the seismic analysis of deep sites," *Soil Dynamics and Earthquake Engrg.*, 22(3), 959-965

Baker, J.W. and C.A. Cornell (2003). "Uncertainty specification and propagation for loss estimation using FOSM methods," *Proceedings, 9th Int. Conf. on Applications of Statistics and Probability in Civil Engineering (ICASP9)*, San Francisco, California: Millpress. 8p.

Chiu, P., D.E. Pradel, A.O.L. Kwok, and J.P. Stewart (2008). "Seismic response analyses for the Silicon Valley Rapid Transit Project," *Proc. 4th Decennial Geotechnical Earthquake Engineering and Soil Dynamics Conference*, ASCE, Sacramento, CA

Chopra, A.K. (2000). *Dynamics of Structures*, 2nd Ed., Prentice Hall

Clough, G.W., and J. Penzien (1993). *Dynamics of Structures*, 2nd Ed., McGraw-Hill, New York.

Darendeli, M. (2001). "Development of a new family of normalized modulus reduction and material damping curves." *Ph.D. Dissertation*, Dept. of Civil Eng., Univ. of Texas, Austin.

Electrical Power Research Institute, EPRI (1993). "Guidelines for determining design basis ground motions," *Rpt. No. EPRI TR-102293*, Palo Alto, CA.

Hardin, B.O. and V.P. Drnevich (1972). "Shear modulus and damping in soils: design equations and curves," J. of the Soil Mechanics and Foundations Div., ASCE, 98 (SM7), 667-692

Hashash, Y.M.A. and D. Park (2001). "Non-linear one-dimensional seismic ground motion propagation in the Mississippi embayment," *Eng. Geology*, 62(1-3), 185-206.

Kausel, E. and D. Assimaki (2002). "Seismic simulation inelastic soils via frequency-dependent moduli and damping." *J. of Engrg. Mech.*, ASCE, 128(1), 34-47.

Kwok, O.A., J.P. Stewart, and, Y.M.A. Hashash (2008) "Nonlinear ground response analysis of Turkey Flat shallow stiff soil site to strong ground motion," *Bull. Seism. Soc. Am.*, 98 (1), in press.

Kwok, O.A., J.P. Stewart, Y.M.A. Hashash, N. Matasovic, R. Pyke, Z. Wang, and Z. Yang (2007). "Use of exact solutions of wave propagation problems to guide implementation of nonlinear seismic ground response analysis procedures," *J. Geotech. & Geoenvir. Engr.,* ASCE, 133 (11), 1385-1398.

Ladd, C.C. (1991). "Stability evaluation during staged construction: 22nd Terzaghi Lecture." *J. Geotech. Engr.*, ASCE, 117(4), 537-615.

Lo Presti, D.C.F., C.G. Lai, and I. Puci (2006). "ONDA: Computer code for nonlinear seismic response analyses of soil deposits." *J. of Geotech. and Geoenvir. Eng.*, ASCE, 132(2), 223-236

Masing, G. (1926). "Eigenspannungen and verfertigung beim messing." *Proc. 2nd Int. Congress on Applied Mech.*, Zurich.

Matasovic, N. and M. Vucetic (1993). "Cyclic Characterization of Liquefiable Sands," *J. of Geotech. Eng.*, ASCE, 119(11), 1805-1822

Melchers, R.E. (1999). *Structural Reliability Analysis and Prediction*. John Wiley and Sons, Chichester.

Park, D. and Y.M.A. Hashash (2004). "Soil damping formulation in nonlinear time domain site response analysis," *J. of Earthquake Eng.,* 8(2), 249-274.

Parra, E. (1996). "Numerical modeling of liquefaction and lateral ground deformation including cyclic mobility and dilation response in soil systemsm" *PhD Dissertation*,

Dept. of Civil Engrg., Rensselaer Polytechnic Institute, Troy, NY.

Pyke, R.M. (1979). "Nonlinear soil models for irregular cyclic loadings," *J. Geotech. Eng.*, ASCE, 105(GT6), 715-726.

Ragheb, A. M. (1994)."Numerical analysis of seismically induced deformations in saturated granular soil strata," *PhD Dissertation*, Dept. of Civil Eng., Rensselaer Polytechnic Institute, Troy, NY.

Seed, H.B. and I.M. Idriss (1970). "Soil moduli and damping factors for dynamic response analyses," *Report EERC 70-10*, Earthquake Engineering Research Center, University of California, Berkeley.

Sheahan, T.C., C.C. Ladd, and J.T. Germaine (1996). "Rate-dependent undrained shear behavior of saturated clay." *Journal of Geotechnical Engineering*, ASCE, 122(2), 99-108

Stewart, J.P., A.O.L. Kwok, Y.M.A. Hashash, N. Matasovic, R. Pyke, Z. Wang, Z. Yang (2007) "Benchmarking of nonlinear grotechnical ground response analysis procedures." *Rpt. No. PEER-2007/XX*, Pacific Earthquake Engineering Research Center, Univ. of California, Berkeley (in press).

Sun, J.I., R. Golesorkhi, and H.B. Seed (1988). "Dynamic moduli and damping ratios for cohesive soils," *Rpt. No. UCB/EERC-88/15*, Earthquake Engineering Research Center, Univ. of California, Berkeley.

Toro, G. R. (1997). ''Probabilistic models of shear-wave velocity profiles at the Savannah River site, South Carolina.'' *Rep. to Pacific Engineering and Analysis*, El Cerrito, Calif.

Vucetic, M. (1990). "Normalized behavior of clay under irregular cyclic loading." *Canadian Geotech. J.*, 27, 29-46.

Vucetic, M. and R. Dobry (1991). "Effect of soil plasticity on cyclic response," *J. Geotech. Engrg.*, ASCE, 117(1), 89-107.

Wang, Z.L. (1990). "Bounding surface hypoplasticity model for granular soils and its applications." *PhD. Dissertation*, Univ. of Calif., Davis

Wang, Z.L., Q.Y. Han, and G.S. Zhou (1980). "Wave propagation method of site seismic response by visco-elastoplastic model," *Proc. of Seventh World Conf.e on Earthquake Eng.*, V2, 379-386

Weiler, W.A. (1988). "Small strain shear modulus of clay," *Proc. of ASCE Conference on Earthquake Engineering and Soil Dynamics II: Recent Advances in Ground Motion Evaluation*, Geotechnical Special Publication 20, ASCE, New York, 331-345.

Yang, Z. (2000). "Numerical modeling of earthquake site response including dilation and liquefaction," *PhD Dissertation*, Dept. of Civil Eng. and Eng. Mech., Columbia University, NY, New York

Youngs, R.R. (2004). *Software validation report for SHAKE04*, Geomatrix Consultants

Zhang, J., R.D. Andrus and C.H. Juang (2005) "Normalized shear modulus and material damping ratio relationships," *J. Geotech. and Geoenvir. Eng.*, ASCE, 131(4), 453-464.